J Gastroenterol (2009) 44:856–863
DOI 10.1007/s00535-009-0075-1

ORIGINAL ARTICLE—LIVER, PANCREAS, AND BILIARY TRACT

Interferon-α-induced mTOR activation is an anti-hepatitis C virus signal via the phosphatidylinositol 3-kinase-Akt-independent pathway

Azusa Matsumoto · Tatsuki Ichikawa · Kazuhiko Nakao · Hisamitsu Miyaaki · Kumi Hirano · Masumi Fujimito · Motohisa Akiyama · Satoshi Miuma · Eisuke Ozawa · Hidetaka Shibata · Shigeyuki Takeshita · Hironori Yamasaki · Masanori Ikeda · Nobuyuki Kato · Katsumi Eguchi

Received: 28 July 2008 / Accepted: 14 April 2009 / Published online: 13 May 2009

Abstract
Object The interferon-induced Jak-STAT signal alone is not sufficient to explain all the biological effects of IFN. The PI3-K pathways have emerged as a critical additional component of IFN-induced signaling. This study attempted to clarify that relationship between IFN-induced PI3-K-Akt-mTOR activity and anti-viral action.
Result When the human normal hepatocyte derived cell line was treated with rapamycin (rapa) before accretion of IFN-α, tyrosine phosphorylation of STAT-1 was diminished. Pretreatment of rapa had an inhibitory effect on the IFN-α-induced expression of PKR and p48 in a dose dependent manner. Rapa inhibited the IFN-α inducible IFN-stimulated regulatory element luciferase activity in a dose-dependent manner. However, wortmannin, LY294002 and Akt inhibitor did not influence IFN-α inducible luciferase activity. To examine the effect of PI3-K-Akt-mTOR on the anti-HCV action of IFN-α, the full-length HCV replication system, OR6 cells were used. The pretreatment of rapa attenuated its anti-HCV replication effect in comparison to IFN-α alone, whereas the pretreatment with PI3-K inhibitors, wortmannin and LY294002 and Akt inhibitor did not influence IFN-induced anti-HCV replication.
Conclusion IFN-induced mTOR activity, independent of PI3K and Akt, is the critical factor for its anti-HCV activity. Jak independent mTOR activity involved STAT-1 phosphorylation and nuclear location, and then PKR is expressed in hepatocytes.

Keywords mTOR · STAT-1 · Interferon · HCV · PKR

Abbreviations

IFN	Interferon
HCV	Hepatitis C virus
STAT	Signal transducers and activators of transcription
ISGF-3	IFN-stimulated gene factor 3
ISRE	IFN-stimulated regulatory element
PKR	Double-stranded RNA-dependent protein kinase
Rapa	Rapamycin
PI3-K	Phosphatidylinositol 3-kinase
mTOR	Mammalian target of rapamycin
siRNA	Small interfering RNA

Introduction

Currently, a chronic hepatitis C virus (HCV) infection is the major cause of hepatocellular carcinoma worldwide [1]. Therefore, an anti-HCV strategy is important for prevention of carcinogenesis. Advancement in the treatment of HCV by a combination of pegylated interferon (IFN) and

A. Matsumoto · K. Hirano
Department of Clinical Pharmaceutics,
Graduate School of Biomedical Sciences,
Nagasaki University, Nagasaki, Japan

T. Ichikawa (✉) · K. Nakao · H. Miyaaki · M. Fujimito · M. Akiyama · S. Miuma · E. Ozawa · H. Shibata · S. Takeshita · K. Eguchi
The First Department of Internal Medicine,
Graduate School of Biomedical Sciences, Nagasaki University,
1-7-1 Sakamoto, Nagasaki 852-8501, Japan
e-mail: ichikawa@net.nagasaki-u.ac.jp

H. Yamasaki
Health Research Center, Graduate School of Biomedical Sciences, Nagasaki University, Nagasaki, Japan

M. Ikeda · N. Kato
Department of Molecular Biology, Graduate School of Medicine and Dentistry, Okayama University, Okayama, Japan

ribavirin is effective in 80% of HCV genotype 2 or 3 cases, but less than 50% of genotype 1 cases. To ameliorate the salvage rate of HCV infection, new anti-HCV agents have been developed to inhibit the life cycle of HCV and are combined with IFN-α [2]. Since IFN-α is the most basic agent for HCV treatment, it is necessary to improvement the salvage rate of HCV infection by clarifying the efficacy of IFN treatment.

The factors associated with a refractory response to IFN treatment are the HCV genotype, viral load, age, sex, fibrosis of the infected liver and metabolic factors such as insulin resistance and steatosis [3]. Increased hepatic expression of the suppressor of cytokine signaling (SOCS) family, known as the Jak-STAT signal inhibitors, especially SOCS-3, is associated with non-response to IFN treatment [4, 5]. It is thought that inflammatory cytokines, such as, interleukin 6, induced by HCV infection can induce SOCS-3 in hepatocyte [5]. SOCS-3 inhibits IFN-induced tyrosine phosphorylation of Jak, then intra-hepatocyte IFN signal transduction is inhibited. For HCV survival, Jak1, Tyk2 and STAT-1,-2 signaling, which is the essential pathway for type 1 IFN-induced anti-viral activity, becomes the attack targets from HCV. The relative lack of a viral response to IFN treatment is associated with blunted IFN signaling [6]. HCV coding proteins also inhibit STAT-1 tyrosine phosphorylation [7]. The cause of a refractory response to IFN treatment is thought to be HCV-induced Jak-STAT signal inhibition.

Type 1 IFN is a pleiotropic cytokine which activates various intra-cellular signal pathways other than the Jak-STAT signal [8]. Additional signaling pathways could either collaborate with STATs at the promoter level and contribute to the activation of the STATs plus transcription factor genes or function totally independent of any STAT factors, thus leading to the activation of transcription factor only genes [8]. The Jak-STAT signal alone is not sufficient to explain all the biological effects of type 1 IFN. The PI3-K and p38 kinase pathways have emerged as critical additional component of IFN-induced signaling [8–10]. p38, activated via IL-1β is enhanced STAT-1 tyrosine phosphorylation and express the anti-viral protein, PKR [9]. The IFN-induced PI3-K-Akt pathway has Jak independent activation, and it is the critical signal for cell survival and insulin action [10], but its relationship with the anti-viral action and PI3-K-Akt pathway is still unclear.

Recently, mTOR, a downstream kinase of PI3-K-Akt pathway, was shown to play a critical role in protein synthesis and anti-viral effects. Kaur and his colleagues [11] reported that the IFN activated mTOR pathway exhibits important regulatory effects in the generation of the IFN responses, including the anti-encephalo myocarditis virus effect. The IFN-induced mTOR is LY294002 sensitive and does not affect the IFN-stimulated regulatory element (ISRE) dependent promoter gene activity. Human cytomegalovirus is inhibited by 5′-AMP-activted protein kinase mediated inhibition of mTOR kinase [12]. In contrast, vesicular stomatitis virus is mTOR dependent [13]. A relationship has been reported between the replication of hepatitis virus and mTOR activity. p21-activated kinase 1 is activated through the mTOR/p70 S6 kinase pathway and regulates the replication of HCV [14]. mTOR activation is dependent upon the PI3-K-Akt and ERK pathways. Gao and colleagues reported that HCV-NS5A protein activates the PI3-K-Akt-mTOR pathway and could inhibit HBV RNA transcription and reduce HBV DNA replication in HepG2 cells [15]. The activation of the N-Ras-PI3-K-Akt-mTOR pathway by HCV is required for cell survival and HCV replication [16]. Therefore, PI3-K, Akt and mTOR activated by HCV are inhibitory signals of HCV replication and survival signals of HCV infected cells. Furthermore, the PI3-K-Akt-mTOR pathway, which is activated by HCV, is thought to be one mechanism for chronic HCV infection [14–16]. However, type 1 IFN-induced PI3-K, Akt and mTOR have not yet been fully evaluated regarding their influence on HCV replication.

This study investigated whether IFN-α induced the PI3-K-Akt-mTOR pathway, whether the Jak-STAT pathway has a relationship with the PI3-K-Akt-mTOR pathway, and, finally, whether IFN induced signal transduction, other than the Jak-STAT pathway, is associated with the anti-HCV activity.

Materials and methods

Reagents and cell culture

Recombinant human IFN-α2b was a generous gift from Schering-Plough KK (Tokyo, Japan). Wortmannin, LY 294002, Akt inhibitor and rapamycin were purchased from Calbiochem (La Jolla, CA, USA). Hc human hepatocyte cells (Applied Cell Biology Research Institute, Kirkland, WA, USA) and HuH-7 human hepatoma cells (American Type Culture Collection, Rockville, MD, USA) were maintained in a chemically defined medium, CS-C completed (Cell Systems, Kirkland, WA, USA) and RPMI (Invitrogen, Grand Island, NY, USA), respectively, supplemented with 5% fetal bovine serum. In the pretreatment of rapamycin and chemical inhibitors for 3 h, the cells were

cultured in 5% RPMI, and then exchanged the medium and treated the cells with IFN-α2b at the indicated time.

Cell viability assay

The cells were measured using the colorimetric cell viability assay method. Cell viability was determined by the colorimetric method using a Cell Counting kit (Wako Life Science, Osaka, Japan). The absorbance of each well was measured at 405 nm with a microtiter plate reader (Multiskan JX, Thermo BioAnalysis Co., Japan). After 2 days of 100 IU/mL IFN-α and 1000 nmol/L rapamycin treatment, Cell viability is expressed as a percentage of the viability in standard media without IFN-α and rapamycin. Data were expressed as the mean ± standard deviation (SD). Statistical significance was assessed using Student's t test. Statistical difference was defined as $P < 0.05$. All numerical results were reported as the mean of four independent experiments.

Western blotting and antibodies

Western blotting with anti-PKR, anti-STAT-1 (Santa Cruz Biotechnology, Santa Cruz, CA, USA), anti-tyrosine-701 phosphorylated STAT-1, anti-serine-727 phosphorylated STAT-1, anti-p48, anti-serine-437 phosphorylated Akt, anti-threonin-308 phosphorylated anti-Akt, anti-Akt, anti-serine-2448 phosphorylated mTOR, anti-serine-2481 phosphorylated mTOR, anti-mTOR, anti-JAK-1 or anti-tyrosine 1022/1023 JAK-1 (Cell Signaling, Beverly, MA, USA) was performed as described previously [9]. Briefly, Hc cells were lysed by the addition of a lysis buffer (50 mmol/L Tris–HCl, pH 7.4, 1% Np40, 0.25% sodium deoxycholate, 0.02% sodium azide, 0.1% SDS, 150 mmol/L NaCl, 1 mmol/L EDTA, 1 mmol/L PMSF, 1 μg/mL each of aprotinin, leupeptin and pepstatin, 1 mmol/L sodium o-vanadate and 1 mmol/L NaF). The samples were separated by electrophoresis on 8–12% SDS polyacrylamide gels and electrotransferred to nitrocellulose membranes, and then blotted with each antibody. The membranes were incubated with horseradish peroxidase-conjugated anti-rabbit IgG or anti-mouse IgG, and the immunoreactive bands were visualized using the ECL chemiluminescence system (Amersham Life Science, Buckinghamshire, England).

Fluorescence immunohistochemistry

The Hc cells were seeded onto 11-mm glass cover-slips in 24-well plates at 2.4×10^5 cells/well. The next day, the medium was replaced with serum-free medium, and the cells were pretreated with 10 or 100 nmol/L rapamycin, or vehicle, for 3 h and then stimulated with 100 IU/mL IFN-α for 10 min. Fluorescence immunohistochemistry was performed as described previously [17]. The cells were incubated with anti-tyrosine-701 phosphorylated STAT1 antibody for 1 h at room temperature, washed three times in PBS, incubated with rhodamine-conjugated donkey anti-rabbit IgG (Jackson ImmunoResearch Laboratories, Inc., West Grove, PA, USA) for 1 h, washed in PBS, and mounted in Vectashield Mounting Medium (Vector Laboratories Inc., Burlingame, CA, USA). Nuclear staining was performed using Hoechst 33258 (Invitrogen Japan K.K., Tokyo, Japan). An immunofluorescence analysis was done using an Olympus BX50 microscope (Tokyo, Japan) and the image was captured by a Nikon DXM 1200 digital camera (Tokyo, Japan).

Reporter gene assay

A pISRE-Luc cis-reporter plasmid containing five copies of the ISRE sequence and the firefly luciferase gene and pRL-SV40 containing the SV40 early enhancer/promoter and the renilla luciferase gene were obtained from Clontech (San Diego, CA, USA) and Promega (Madison, WI, USA), respectively. The HuH-7 cells were grown in 24-well multiplates and transfected with 1 μg of pISRE-Luc and 10 ng of pRL-SV40 as a standard by the lipofection method. One day later, the cells were incubated in the absence or presence of varying concentrations of chemical blockers and IFN-α, and the luciferase activities in the cells were determined using a dual-luciferase reporter assay system and a TD-20/20 luminometer (Promega). The data were expressed as the relative ISRE-luciferase activity.

HCV replicon system

OR6 cells stably harboring the full-length genotype 1 replicon, ORN/C-5B/KE [18], were used to examine the influence of the anti-HCV effect of IFN. The cells were cultured in Dulbecco's modified Eagle's medium (Gibco-BRL, Invitrogen) supplemented with 10% fatal bovine serum, penicillin and streptomycin and maintained in the presence of G418 (300 mg/L; Geneticin, Invitrogen). This replicon was derived from the 1B-2 strain (strain HCV-o, genotype 1b), in which the *Renilla* luciferase gene is introduced as a fusion protein with neomycin to facilitate the monitoring of HCV replication. After the treatment, the cells were harvested with *Renilla* lysis reagent (Promega, Madison, WI, USA) and then were subjected to a luciferase assay according to the manufacturer's protocol. mTOR gene knock down is used siRNA (Cell Signaling). 100 nmol/L mTOR specific and non-targeted siRNA as a control was transfected to OR6 cells in accordance with the appended manual. One day later, the cells were incubated in either the absence or presence of 10 IU/mL IFN-α.

Results

IFN-α-induced activity of STAT-1 is inhibited by rapamycin pretreatment

To attempt to clearly identify the influence of mTOR to IFN-α-induced anti-viral protein expression rapamycin (rapa), the specific inhibitor of mTOR, was added prior to treatment with IFN-α. Hc cells have been used as normal hepatocytes in previous reports [19]. The Hc cells were incubated in the absence or presence of IFN-α with or without pretreatment with rapa for 2 h the cells were then harvested for the Western blot analysis (Fig. 1). IFN-α clearly induced tyrosine and serine phosphorylation of STAT-1 at 5 (Fig. 1a, lane 4) and 10 min (Fig. 1a, lane 6), respectively, in the absence of rapa. However, when the Hc cells were pretreated with rapa before IFN-α stimulation, the levels of tyrosine and serine phosphorylated STAT-1 were clearly and rapidly lower than those induced by IFN-α alone 5 min after treatment in tyrosine (Fig. 1a, lane 5). Jak-1, an upstream protein of STAT-1, was equally phosphorylated by IFN-α with (Fig. 1b, lane3) or without (Fig. 1b, lane2) pretreatment with rapa. The viability of the Hc cells was 1 in vehicle, 0.93±0.21 in IFN-α treatment and 0.88±0.34 in rapamycin treatment. No difference in the cell viability the among vehicle, IFN-α and rapamycin treatment was not recognized in our assay. The viability of the HuH-7 and OR6 cells also demonstrated no difference between the presence of IFN-α and rapamycin treatment and the absence thereof.

IFN inducible gene products are diminished by pretreatment of rapamycin

Since pretreatment with rapa inhibited the IFN-α induced STAT-1 activity, the phosphorylation of tyrosine and serine and nuclear translocation, the effect of pretreated with rapa on the IFN-α inducible gene product was examined. The protein levels of PKR, an anti-viral protein that acts as a mRNA translation inhibiter activated by double stranded RNA [20, 21], and p48, key component of ISGF-3 with activated STAT-1 and -2 [22], were induced by IFN-α treatment for 3 h in Hc cells (Fig. 1c, lanes 1, 2). However, pretreatment with rapa had an inhibitory effect on IFN-α-induced PKR and p48 in a dose dependent manner (Fig. 1c, lanes 2–4).

The serine 473 on Akt and serine 2448 on mTOR are phosphorylated by IFN-α

Because pretreatment with rapa affected the IFN-α signaling (Fig. 1), the ability of IFN-α to activate the Akt-mTOR pathway was investigated. The phosphorylation of serine-2448 residues of mTOR and serine-473 residue of

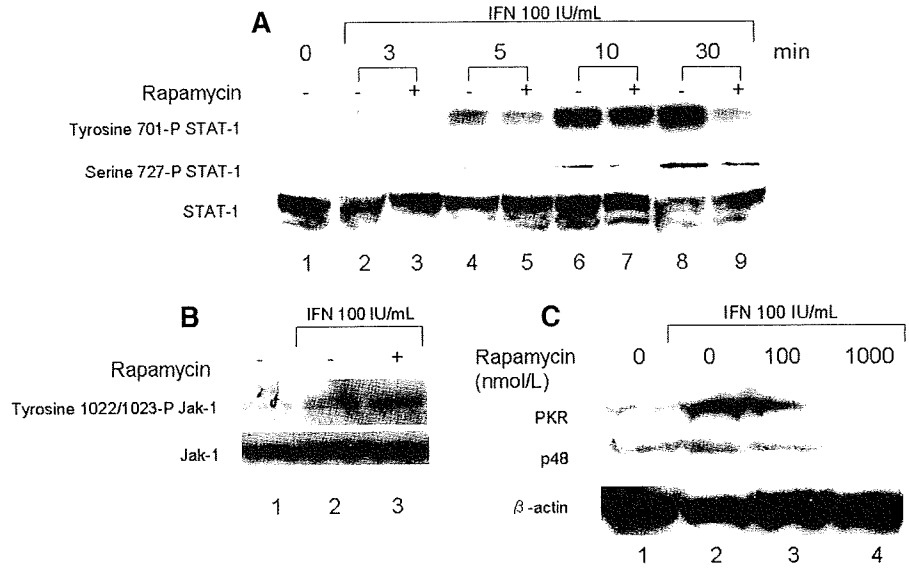

Fig. 1 Alteration in the distribution of IFN-α induced phosphorylated STAT-1 (**a**) and Jak-1 (**b**) by rapamycin and effect of rapamycin on IFN-α-induced PKR and p48 (**c**). Hc cells were pretreated without (*lanes 1, 2, 4, 6,* and *8*) or with 1 μmol/L rapa (*lanes 3, 5, 7,* and *9*). These Hc cells were stimulated by 100 IU/L IFN-α (*lane 2–9*) for 30 min. Phosphorylated STAT-1 at tyrosine-701 residue (*upper panel*) and at serine-727 residue (*lower panel*) were analyzed by Western blotting. **a** After pretreatment of 1000 nmol/L rapa (*lane 3*) for 3 h, Hc cells were untreated (*lane 1*) or treated with 100 IU/mL IFN-α (*lanes 2, 3*) for 3 min, then phosphorylated JAK-1 at tyrosine-1022/1023 residue (*first panel*), expression of JAK-1 (*second panel*) were analyzed by Western blotting (**b**). Hc cells were treated with 100 IU/mL of IFN-α in the absence (*lane 2*) or of the presence of pretreatment (*lane 3, 4*). *Lane 1* was not treated IFN-α and calcineurin inhibitors. One day latter, PKR and p48 was determined by Western blotting (**c**)

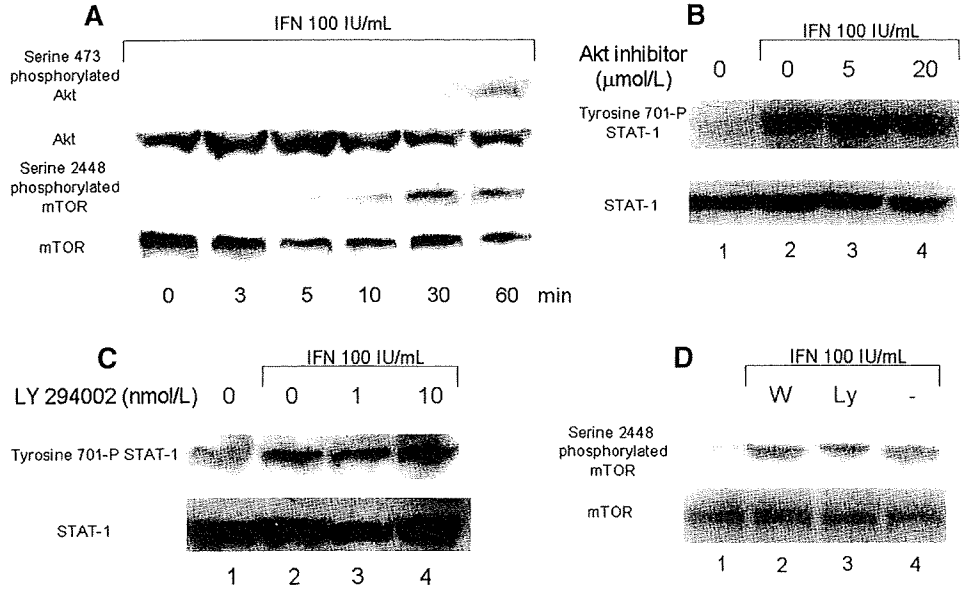

Fig. 2 Effect of IFN-α on Akt and mTOR (**a**) and effect of Akt inhibitor (**b**) and LY294002 (**c**) on IFN-α-induced tyrosine phosphorylated STAT-1 and Serine phosphorylated mTOR (**d**). Hc cells were stimulated by 100 IU/L IFN-α for 60 min. At the indicated time, the cells were harvested. Phosphorylated Akt at serine-473 residue (*first panel*), Akt (*second panel*), mTOR at serine-2448 residue (*third panel*) and mTOR (*fourth panel*) were analyzed by Western blotting. After pretreatment with 5 or 20 μmol/L Akt inhibitor (*lane 3*, and 4, respectively) (**b**) and 1 or 10 nmol/L LY294002 (*lane 3* and *4*, respectively) (**c**) for 3 h, Hc cells were untreated (*lane 1*) or treated with 100 IU/mL IFN-α (*lanes 2–4*) for 5 min and phosphorylated STAT-1 at tyrosine-701 residue (*first panel*), expression of STAT-1 (*second panel*) were analyzed by Western blotting. **d** After pretreatment with 100 nmol/L wortmannin (*lane 2*) and 1 nmol/L LY294002 (*lane 3*) for 3 h, the Hc cells were either untreated (*lane 1*) or treated with 100 IU/mL IFN-α (*lanes 2–4*) for 10 min and then were phosphorylated mTOR at Serine-2448 residue (*first panel*), the expression of mTOR (*second panel*) was analyzed by Western blotting

Akt by 100 IU/ml of IFN-α was detected at 5 min and at 60 min after IFN-α treatment, respectively (Fig. 2a). The band intensity of serine 2448 phosphorylated mTOR increased at 30 min and decreased at 60 min after IFN-α treatment. In contrast, a slight band intensity of serine phosphorylated 473 Akt was only detected at 60 min after IFN-α treatment. In addition, a Western blot analysis of phosphorylated serine 2481 of mTOR and threonine 308 Akt was conducted under the same conditions as Fig. 2a, but no bands were detected (data not shown). In Fig. 2d, IFN-α-induced Serine 2448 phosphorylated mTOR was not inhibited by PI3-K inhibitors (lanes 2, 3).

The IFN-α-induced nuclear translocation of tyrosine phosphorylated STAT-1 was inhibited by pretreatment with rapa

The location of tyrosine phosphorylated STAT-1 was evaluated by fluorescence immunohistochemistry of cultured Hc cells (Fig. 3). The IFN-α-induced nuclear translocation of tyrosine phosphorylated STAT-1 was observed (Fig. 3c), but its translocation was inhibited by pretreatment with rapa and the inhibition of the translocation of STAT-1 was more definitive at 1000 nmol/L rapa (Fig. 3e) than 100 nmol/L (Fig. 3g).

IFN-α-induced ISRE-contained promoter activity is inhibited by pretreatment of rapa, but not by wortmannin, LY294002 and Akt inhibitor

The influence of pretreatment of PI3-K-Akt-mTOR inhibitors on IFN-α inducible luciferase activity of the ISRE-containing promoter was examined. Since Hc cells were not sufficient for reporter gene transfection, HuH-7 cells were used in the transfection assay. HuH-7 cells were transfected with pISRE-Luc containing five repeats of the ISRE sequence and pRV-SV40 as a standard and then were treated with IFN-α after 3 h with or without pretreatment with rapa, wortmannin, LY294002 or Akt inhibitor. Rapa inhibited IFN-α inducible luciferase activity in a dose-dependent manner (Fig. 4, lane 2–4). However, wortmannin and LY294002, PI3-K inhibitor, and Akt inhibitor had no effect on IFN-α inducible luciferase activity (Fig. 4, lanes 2, 5–7).

The expression of IFN-α-induced tyrosine phosphorylated STAT-1 was determined after pretreatment with Akt inhibitor and LY294002 to evaluate the result of luciferase assay (Fig. 4). The Hc cells were incubated under the same conditions used in Fig. 4, but phosphorylated STAT-1 was not inhibited by the Akt inhibitor (Fig. 2b) and LY294002 (Fig. 2c).

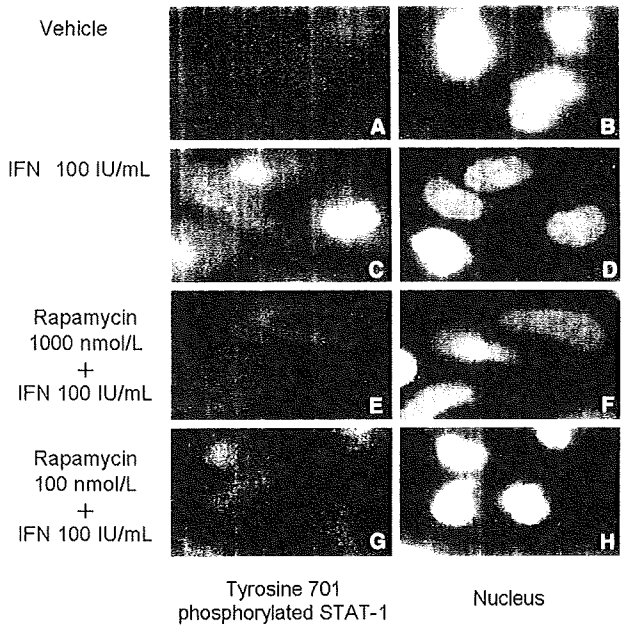

Fig. 3 Inhibition of IFN-α-induced nuclear translocation of phosphorylated STAT-1 by rapamycin. The Hc cells were pretreated without (**a**–**d**) or with 1000 nmol/L rapa (**e**, **f**) or 100 nmol/L rapa (**g**, **h**). After pretreatment, the Hc cells were stimulated by 100 IU/L IFN-α (**c**–**h**) for 30 min. Thereafter, the cells were fixed, permeabilized, processed for immunofluorescence (**a**, **c**, **e**, **g**) and Hoechst staining (**b**, **d**, **f**, **h**), and visualized by fluorescence microscopy. The results shown are from one representative experiment from a total of three performed

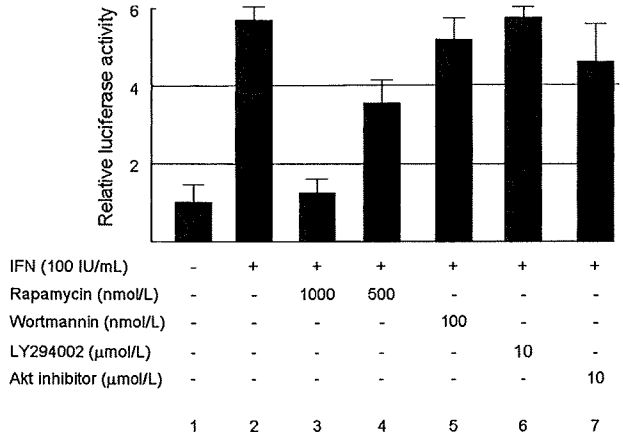

Fig. 4 Suppression effect of rapamycin, not PI3-k inhibitors and Akt inhibitor, on IFN-α-induced reporter gene assay. HuH-7 cells transfected with reporter gene (pISRE-Luc and pRL-SV40) were either untreated (*lane 1*) or pretreated with rapa (*lane 3*, *4*), wortmannin (*lane 5*), LY294002 (*lane 6*) or Akt inhibitor (*lane 7*) for 3 h, followed by IFN-α 100 IU/mL (*lanes 2–7*). Six hour later, the relative ISRE-luciferase activity ($n = 4$) was determined as described in the "Materials and methods". The data are expressed as the mean ± SD and are representative example of four similar experiments

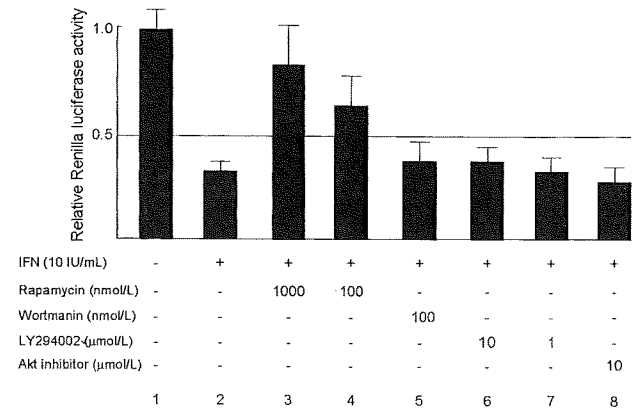

Fig. 5 Alternation of IFN-α suppressed HCV replication by rapamycin, but not PI3-K inhibitors and Akt inhibitor. OR6 cells, a full-length replicon system, were treated with 100 IU/mL of IFN-α in the absence (*lane 2*) or presence of pretreatment (*lanes 3–8*) for 3 h. *Lane 1* was not treated IFN-α alone. One day latter, *Renilla* luciferase activity was determined by luminometer ($n = 4$). The data are expressed as the mean ± SD and are representative example of four similar experiments

Rapamycin and mTOR specific siRNA, but not PI3-K inhibitor and Akt inhibitor can cancel the IFN-α-induced anti-HCV replicon activity

OR6 cells the full-length HCV replication system was used to examine the anti-viral effect of PI3-K, Akt and mTOR on IFN-α stimulation. The cells were treated with IFN-α after 3 h in the presence or absence of rapa, Akt inhibitor or PI3-K inhibitor (Fig. 5). Pretreatment with rapa attenuated its anti-HCV replication effect in comparison to IFN-α alone (Fig. 5, lanes 1–4), whereas pretreatment with PI3-K inhibitors and Akt inhibitor did not increase the *Renilla* luciferase activity (Fig. 5, lanes 1, 2, 5–8). We performed siRNA transfection for mTOR knock down (Fig. 6). Although transfection efficiency of siRNA is barely 10%, IFN-α-induced anti-HCV action was clearly inhibited in siRNA against mTOR transfected cells (lane 5) in comparison to the control cells (lane 6).

Discussion

Rapa inhibited the IFN-α-induced tyrosine and serine phosphorylation and nuclear translocation of STAT-1, the ISRE-promoter activity, the expression of PKR and the replication of HCV replicon. This suggests that the IFN-induced mTOR activity, through Jak independent STAT-1 phosphorylation, is a critical signal for IFN-induced anti-HCV action. Interestingly, mTOR activated by IFN was PI3-K-Akt independent in this study.

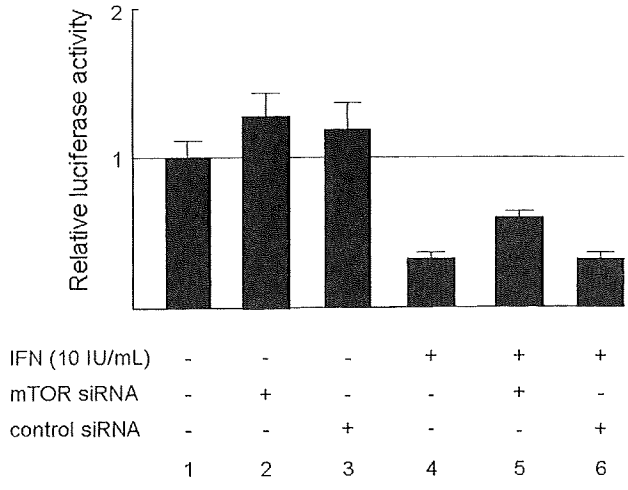

Fig. 6 Alternation of IFN-α suppressed HCV replication by siRNA against mTOR. The OR6 cells were transfected the siRNA against mTOR (*lanes 2, 5*) and the non-targeted siRNA (*lanes 3, 6*). One day later, the cells were IFN-α treatment (*lanes 4–6*). HCV replicon assay is same as Fig. 5. The data are expressed as the mean ± SD and are representative example of four similar experiments

mTOR activity may have an inhibitory action on HCV replication through STAT-1 phosphorylation, but not the translation initiation action of mTOR. This study assumed that IFN-induced PKR expression and ISRE-luciferase activity were inhibited by rapa as the result of a suppression effect on IFN inducible STAT-1 activation. IFN inducible PKR contributes the anti-HCV action [20], and anti-HCV action of ribavirin is also attributable to its ability to up-regulate PKR activity [21]. Previous reports revealed that the mTOR activity did not influence the HCV-IRES activity because the viral promoter has cap-independent translation [23]. Although mTOR is the mRNA translational regulator through phosphorylation of a downstream target such as 4E-BP and S6K [24], we think that the IFN-induced mTOR activity influences the phosphorylation of STAT-1 in our study (Fig. 1). In addition, it is thought that the alternation of STAT-1 phosphorylation by the mTOR activity influences the gene expression of anti-virus protein and IFN-induced anti-viral action.

In our study, serine-473 on Akt showed a delayed phosphorylation in comparison to that of serine-2448 on mTOR after IFN stimulation (Fig. 2a). Since serine-473 on Akt is phosphorylated by mTOR/Rictor/GβL [25, 26] and a PDK-1 independent pathway [25], IFN-induced serine-473 phosphorylated Akt may not involve the mTOR activity. Therefore, PI3-K inhibitor and Akt inhibitor had no effect on IFN inducible anti-HCV action. The pathway of mTOR activation is prismatic. PI-3Ks, upstream kinase of Akt and mTOR, are grouped into three classes (I–III), according to their substrate preference and sequence homology [27]. PI3-k inhibitor, wortmannin and LY294002, inhibit class I and III PI3-Ks, and to a lesser extent class II PI3-K, upstream kinase of Akt [27]. In our study, neither PI3-K nor Akt inhibitor inhibited IFN-induced ISRE luciferase activity and loss of HCV replication (Figs. 4, 5). These results indicate that the IFN-induced anti-HCV activity is mTOR dependent, but not PI3-K and Akt dependent. In the current report, the production of IL-1 receptor antagonist in IFN-stimulated monocytes depends on the PI3-K pathway, but not STAT-1 [28], and chronic myelogenous leukemia cells are differentially regulated by the IFN-induced PI3-K-Akt-mTOR pathway with no relation to STAT-1 phosphorylation [29]. Similar to the findings of those reports, the PI3-K-Akt pathway has been reported to be generally independent of the STAT activity [10]. Therefore, the difference in the cell type [8] may explain the discrepancy between these data and our data. We therefore speculate that in hepatocytes, unlike lymphoid cells, IFN-induced mTOR activity is not dependent on the PI3-K activity. In addition, the mTOR activity is not related to the STAT activity in lymphoid cells. However, in hepatocytes, the IFN-induced mTOR activity was closely linked to the IFN-induced STAT activity in our study.

mTOR is a serine and threonine kinase [10]. Phosphorylation of STATs by mTOR occurs also on a serine residue, but not tyrosine [10, 30]. The mTOR pathway is critical for IFN-γ-induced suppression of tyrosine phosphorylated STAT-3 in a prostate cancer cell line [31]. Although this is not consistent with the results of our study, this also showed mTOR to be associated with tyrosine phosphorylation without reference to SOCS and phosphatase. In addition, in a mouse embryo fibroblast cell line, IFN-γ-induced tyrosine and serine phosphorylation of STAT-1 is inhibited by rapa [32], while in the hepatoma cell line, HLF, IFN-β stimulated STAT-1 tyrosine phosphorylation partially decreases by LY294002, but the effect of rapa has not yet been studied [33]. In the current study [31–33], not only STAT-1 serine phosphorylation but also tyrosine was found to be downstream of the IFN induced mTOR activity; however, the mechanism controlling the tyrosine phosphorylation of STAT-1 and the mTOR activity, remains to be elucidated.

In conclusion, IFN-induced mTOR activity, independent of PI3-K and Akt, is the critical factor for anti-HCV action. The Jak independent mTOR activity is, therefore, involved in STAT-1 phosphorylation and nuclear location, thus resulting in the development of IFN-induced anti-HCV protein, especially the expression of PKR, in HCV-infected hepatocytes.

References

1. Fattovich G, Stroffolini T, Zagni I, Donato F. Hepatocellular carcinoma in cirrhosis: incidence and risk factors. Gastroenterology. 2004;127:S35–50.
2. Pawlotsky JM, Chevaliez S, McHutchison JG. The hepatitis C virus life cycle as a target for new antiviral therapies. Gastroenterology. 2007;132:1979–98.
3. Persico M, Capasso M, Persico E, Svelto M, Russo R, Spano D, et al. Suppressor of cytokine signaling 3 (SOCS3) expression and hepatitis C virus-related chronic hepatitis: insulin resistance and response to antiviral therapy. Hepatology. 2007;46:1009–15.
4. Walsh MJ, Jonsson JR, Richardson MM, Lipka GM, Purdie DM, Clouston AD, et al. Non-response to antiviral therapy is associated with obesity and increased hepatic expression of suppressor of cytokine signaling 3 (SOCS-3) in patients with chronic hepatitis C, viral genotype 1. Gut. 2006;55:529–35.
5. Huang Y, Feld JJ, Sapp RK, Nanda S, Lin JH, Blatt LM, et al. Defective hepatic response to interferon and activation of suppressor of cytokine signaling 3 in chronic hepatitis C. Gastroenterology. 2007;132:733–44.
6. Taylor MW, Tsukahara T, Brodsky L, Schaley J, Sanda C, Stephens MJ, et al. Changes in gene expression during pegylated interferon and ribavirin therapy of chronic hepatitis C virus distinguish responders from nonresponders to antiviral therapy. J Virol. 2007;81:3391–401.
7. Lan KH, Lan KL, Lee WP, Sheu ML, Chen MY, Lee YL, et al. HCV NS5A inhibits interferon-alpha signaling through suppression of STAT1 phosphorylation in hepatocyte-derived cell lines. J Hepatol. 2007;46:759–67.
8. van Boxel-Dezaire AH, Rani MR, Stark GR. Complex modulation of cell type-specific signaling in response to type I interferons. Immunity. 2006;25:361–72.
9. Ichikawa T, Nakao K, Nakata K, Yamashita M, Hamasaki K, Shigeno M, et al. Involvement of IL-1beta and IL-10 in IFN-alpha-mediated antiviral gene induction in human hepatoma cells. Biochem Biophys Res Commun. 2002;294:414–22.
10. Kaur S, Uddin S, Platanias LC. The PI3' kinase pathway in interferon signaling. J Interferon Cytokine Res. 2005;25:780–7.
11. Kaur S, Lal L, Sassano A, Majchrzak-Kita B, Srikanth M, Baker DP, et al. Regulatory effects of mammalian target of rapamycin-activated pathways in type I and II interferon signaling. J Biol Chem. 2007;282:1757–68.
12. Kudchodkar SB, Del Prete GQ, Maguire TG, Alwine JC. AMPK-mediated inhibition of mTOR kinase is circumvented during immediate-early times of human cytomegalovirus infection. J Virol. 2007;81:3649–51.
13. Minami K, Tambe Y, Watanabe R, Isono T, Haneda M, Isobe K, et al. Suppression of viral replication by stress-inducible GADD34 protein via the mammalian serine/threonine protein kinase mTOR pathway. J Virol. 2007;81:11106–15.
14. Ishida H, Li K, Yi M, Lemon SM. p21-activated kinase 1 is activated through the mammalian target of rapamycin/p70 S6 kinase pathway and regulates the replication of hepatitis C virus in human hepatoma cells. J Biol Chem. 2007;282:11836–48.
15. Guo H, Zhou T, Jiang D, Cuconati A, Xiao GH, Block TM, et al. Regulation of hepatitis B virus replication by the phosphatidylinositol 3-kinase-Akt signal transduction pathway. J Virol. 2007;81:10072–80.
16. Mannova P, Beretta L. Activation of the N-Ras-PI3K-Akt-mTOR pathway by hepatitis C virus: control of cell survival and viral replication. J Virol. 2005;79:8742–9.
17. Nishimura D, Ishikawa H, Matsumoto K, Shibata H, Motoyoshi Y, Fukuta M, et al. DHMEQ, a novel NF-kappaB inhibitor, induces apoptosis and cell-cycle arrest in human hepatoma cells. Int J Oncol. 2006;29:713–9.
18. Ikeda M, Abe K, Dansako H, Nakamura T, Naka K, Kato N. Efficient replication of a full-length hepatitis C virus genome, strain O, in cell culture, and development of a luciferase reporter system. Biochem Biophys Res Commun. 2005;329:1350–9.
19. Obora A, Shiratori Y, Okuno M, Adachi S, Takano Y, Matsushima-Nishiwaki R, et al. Synergistic induction of apoptosis by acyclic retinoid and interferon-beta in human hepatocellular carcinoma cells. Hepatology. 2002;36:1115–24.
20. Wang C, Pflugheber J, Sumpter R Jr, Sodora DL, Hui D, Sen GC, et al. Alpha interferon induces distinct translational control programs to suppress hepatitis C virus RNA replication. J Virol. 2003;77:3898–912.
21. Liu WL, Su WC, Cheng CW, Hwang LH, Wang CC, Chen HL, et al. Ribavirin up-regulates the activity of double-stranded RNA-activated protein kinase and enhances the action of interferon-alpha against hepatitis C virus. J Infect Dis. 2007;196:425–34.
22. Tamada Y, Nakao K, Nagayama Y, Nakata K, Ichikawa T, Kawamata Y, et al. p48 Overexpression enhances interferon-mediated expression and activity of double-stranded RNA-dependent protein kinase in human hepatoma cells. J Hepatol. 2002;37:493–9.
23. Dowling RJ, Zakikhani M, Fantus IG, Pollak M, Sonenberg N. Metformin inhibits mammalian target of rapamycin-dependent translation initiation in breast cancer cells. Cancer Res. 2007;67:10804–12.
24. Mamane Y, Petroulakis E, LeBacquer O, Sonenberg N. mTOR, translation initiation and cancer. Oncogene. 2006;25:6416–22.
25. Hanada M, Feng J, Hemmings BA. Structure, regulation and function of PKB/AKT–a major therapeutic target. Biochim Biophys Acta. 2004;1697:3–16.
26. Hresko RC, Mueckler M. mTOR.RICTOR is the Ser473 kinase for Akt/protein kinase B in 3T3–L1 adipocytes. J Biol Chem. 2005;280:40406–16.
27. Engelman JA, Luo J, Cantley LC. The evolution of phosphatidylinositol 3-kinases as regulators of growth and metabolism. Nat Rev Genet. 2006;7:606–19.
28. Molnarfi N, Hyka-Nouspikel N, Gruaz L, Dayer JM, Burger D. The production of IL-1 receptor antagonist in IFN-beta-stimulated human monocytes depends on the activation of phosphatidylinositol 3-kinase but not of STAT1. J Immunol. 2005;174:2974–80.
29. Parmar S, Smith J, Sassano A, Uddin S, Katsoulidis E, Majchrzak B, et al. Differential regulation of the p70 S6 kinase pathway by interferon alpha (IFNalpha) and imatinib mesylate (STI571) in chronic myelogenous leukemia cells. Blood. 2005;106:2436–43.
30. Nguyen H, Ramana CV, Bayes J, Stark GR. Roles of phosphatidylinositol 3-kinase in interferon-gamma-dependent phosphorylation of STAT1 on serine 727 and activation of gene expression. J Biol Chem. 2001;276:33361–8.
31. Fang P, Hwa V, Rosenfeld RG. Interferon-gamma-induced dephosphorylation of STAT3 and apoptosis are dependent on the mTOR pathway. Exp Cell Res. 2006;312:1229–39.
32. El-Hashemite N, Zhang H, Walker V, Hoffmeister KM, Kwiatkowski DJ. Perturbed IFN-gamma-Jak-signal transducers and activators of transcription signaling in tuberous sclerosis mouse models: synergistic effects of rapamycin-IFN-gamma treatment. Cancer Res. 2004;64:3436–43.
33. Matsumoto K, Okano J, Murawaki Y. Differential effects of interferon alpha-2b and beta on the signaling pathways in human liver cancer cells. J Gastroenterol. 2005;40:722–32.

Clinicopathological study of hepatocellular carcinoma with peliotic change

MASARU FUJIMOTO[1,2], OSAMU NAKASHIMA[1], MINA KOMUTA[1], TOSHIMITSU MIYAAKI[1], MASAMICHI KOJIRO[1] and HIROHISA YANO[1]

[1]Department of Pathology, Kurume University School of Medicine, Kurume, Fukuoka 830-0011; [2]Division of Hepatology and Metabolism, Department of Internal Medicine, Faculty of Medicine, Saga University, Nabeshima 849-8501, Japan

Received May 25, 2009; Accepted September 23, 2009

DOI: 10.3892/ol_00000003

Abstract. Peliosis hepatis-like blood-filled cavities are frequently observed in the tumors of hepatocellular carcinoma (HCC). This finding is generally referred to as 'peliotic change' in HCC. However, the clinicopathological features of HCC with peliotic change (PHCC) are not fully understood. These issues are addressed in the present study. Among 294 consecutively surgically resected HCCs, the clinicopathological features of PHCC were compared with those of a common type of HCC (control). PHCC was observed in 116 (39.5%) of 294 HCCs. The mean tumor diameter of 3.4±0.9 cm of the PHCC group was significantly larger than that of the 2.5±0.9 cm of the control, and the incidence of PHCC was related to increased tumor diameter. In the 116 PHCCs, the tumors were completely or incompletely encapsulated. On ultrasonography, PHCCs showed hyperechoic and/or mosaic patterns. The mean diameter of 3.5±0.8 cm of PHCCs with a hyperechoic and/or mosaic pattern was significantly larger than that of 2.3±0.9 cm in the control. In conclusion, it is necessary for clinicians and pathologists to discern the characteristics of peliotic change as a morphological feature that modifies ultrasound findings.

Introduction

Peliosis hepatis, a hepatic lesion characterized by blood-filled parenchymal cavities randomly scattered throughout the liver (1-3), was first described by Wagner (4), but its pathogenesis is a matter of debate. Peliosis hepatis-like blood-filled cavities are also frequently observed in the tumors of hepatocellular carcinoma (HCC) (5-7). This finding is generally referred to as 'peliotic change' in HCC. Almost no clinicopathological assessment of this peliotic change has been conducted, and it is still considered little more than an often observed incidental or accidental finding. However, along with the advances in diagnostic imaging, peliotic change has drawn attention as a morphological feature that modifies image findings of HCC.

In the present study, we conducted a clinicopathological study of HCC with peliotic change (PHCC).

Materials and methods

A total of 294 HCCs without preoperative anticancer therapies were consecutively resected at Kurume University Hospital between January 1991 and December 2003. Cases showing a peliosis hepatis-like change (peliotic change) in the tumor were included for the study as PHCC and compared with cases of a common type of HCC as control. The resected liver specimens were fixed in 10% buffered formalin immediately after hepatectomy, cut serially into 5 mm slices and macroscopically examined. Sections containing tumor tissues as well as the surrounding liver tissues were embedded in paraffin, cut into 4-μm sections and routinely stained with hematoxylin and eosin. Immunohistochemical staining of CD34 was performed on 20 PHCC cases to examine the endothelial cells of the sinusoidal blood spaces of the tumor, using mouse monoclonal antibody against CD34 (anti-CD34; Dako, CA, USA) and the Streptavidin Peroxidase technique (MaxiTags kits, Immunon™, Lipshaw, PA, USA). Clinical data were obtained from clinical charts. Informed consent was obtained from the patients included in the study.

Statistical analysis was performed using Stat View version J-5.0 (Abacus Concepts Inc., Berkeley, CA, USA). Difference of means was assessed by the unpaired Student's t-test or Mann-Whitney U test. $P<0.05$ was considered statistically significant.

Results

Clinical findings of PHCC. PHCC was observed in 116 (39.5%) out of 294 cases. Ages ranged from 41 to 78 years (mean 63.2±7.8 SD) in the PHCCs and from 16 to 80 years (mean 64.5±8.8 SD) in the control group. The PHCC group

Correspondence to: Dr Hirohisa Yano, Department of Pathology, Kurume University School of Medicine, 67 Asahi-machi, Kurume, Fukuoka 830-0011, Japan
E-mail: hiroyano@med.kurume-u.ac.jp

Key words: hepatocellular carcinoma, peliotic change, peliosis hepatis, ultrasound, mosaic pattern

Table I. Comparison of the ultrasonographic pattern between hepatocellular carcinoma with peliotic change and a common type of HCC (control) according to the tumor size.

Tumor size (cm)	0.0-1.0	1.1-2.0	2.1-3.0	3.1-4.0	4.1-5.0	Total (%)
PHCC group						
Hyperechoic	0	0	3	5	4	12 (20)
Mosaic	0	1	7	5	5	18 (31)[a]
Isoechoic	0	2	2	2	2	8 (14)
Hypoechoic	0	4	7	10	0	21 (36)
Total	0	7	19	22	11	59 (100)
Control group						
Hyperechoic	3	7	6	1	0	17 (19)
Mosaic	0	3	6	1	1	11 (13)
Isoechoic	2	3	6	5	2	18 (20)
Hypoechoic	2	17	19	4	0	42 (48)
Total	7	30	37	11	3	88 (100)

[a]P<0.01 vs. mosaic in control.

included 89 males and 27 females (3.3:1), while the control group comprised 140 males and 38 females (3.7:1). No significant difference was noted in gender between the two groups.

Hepatitis B surface antigen (HBsAg) was found to be positive in 16 cases (15%) out of 104 in the PHCC group and in 20 cases (12%) out of 163 in the control group. Hepatitis C virus antibody (HCVAb) was found to be positive in 82 cases (77%) out of 107 in the PHCC group and in 132 cases (80%) out of 166 cases in the control group, indicating no significant difference between the two groups. In the remaining 27 and 21 of the 294 cases, respectively, HBsAg- and HCVAb-positives were unknown.

The laboratory data for asparate aminotransferase, alanine aminotransferase, albumin, as well as platelet and serum α-fetoprotein were not significantly different between the two groups.

Imaging findings of PHCC. Among 59 PHCCs in which abdominal ultrasound findings were available, 12 (20%) had a hyperechoic pattern and 18 (31%) a mosaic pattern. Among 88 cases of the control group, 17 (19%) had a hyperechoic pattern and 11 (13%) a mosaic pattern, indicating significantly more lesions with a mosaic pattern in the PHCC group (P<0.01; Table I). Furthermore, the mean tumor diameter in the cases with a hyperechoic pattern and/or mosaic pattern was 3.5±0.8 cm in the PHCC group and 2.3±0.9 cm in 28 controls. The tumor size of PHCCs with hyperechoic and/or mosaic patterns was significantly larger than that of the control (P<0.001).

In the majority of 50 cases in the PHCC group that underwent dynamic CT scans, typical HCC patterns were observed, such as high attenuation in the early enhanced phase and wash-out in the delay enhanced phase. No specific difference in CT findings was noted in PHCCs.

Pathological findings of PHCC. Tumor diameter ranged from 1.5 to 5.0 cm (average 3.4±0.9 SD) in the PHCC group and from 0.7 to 4.8 cm (average 2.5±0.9 SD) in the control group, indicating significantly larger tumors in the PHCC group (P<0.001; Table II). The incidence of PHCC was related to the increase of tumor diameter. Tumors <2 cm were found in 10 cases (9%) in the PHCC group and in 65 cases (37%) in the control. No tumors <1 cm in diameter were detected in the PHCC group.

Table II. Comparison in tumor size between hepatocellular carcinoma with peliotic change and a common type of HCC (control).

Tumor size (cm) Average ± SD	PHCC (%) 3.4±0.9[a]	Control (%) 2.5±0.9
0.0-1.0	0 (0)	11 (100)
1.1-2.0	10 (16)	54 (84)
2.1-3.0	37 (32)	77 (68)
3.1-4.0	44 (61)	28 (39)
4.1-5.0	25 (76)	8 (24)
Total	116 (100)	178 (100)

[a]P<0.001 vs. control.

The tumors were completely encapsulated in 108 (93%) of the 116 PHCCs, but incompletely encapsulated in the remaining 8 cases. On the other hand, encapsulated HCC was observed in 106 (60%) out of 178 tumors in the control group, indicating a significantly higher frequency of encapsulation in the PHCC group (P<0.001). Peliotic change was observed as varying sized blood lakes and hemorrhagic honeycomb-like appearance (Fig. 1A and B). In some cases, peliotic changes occupied ~2/3 of the cut surface of the tumor. Peliotic changes were easily distinguished from hemorrhage because the latter was accompanied by degeneration and/or necrosis of the tumor

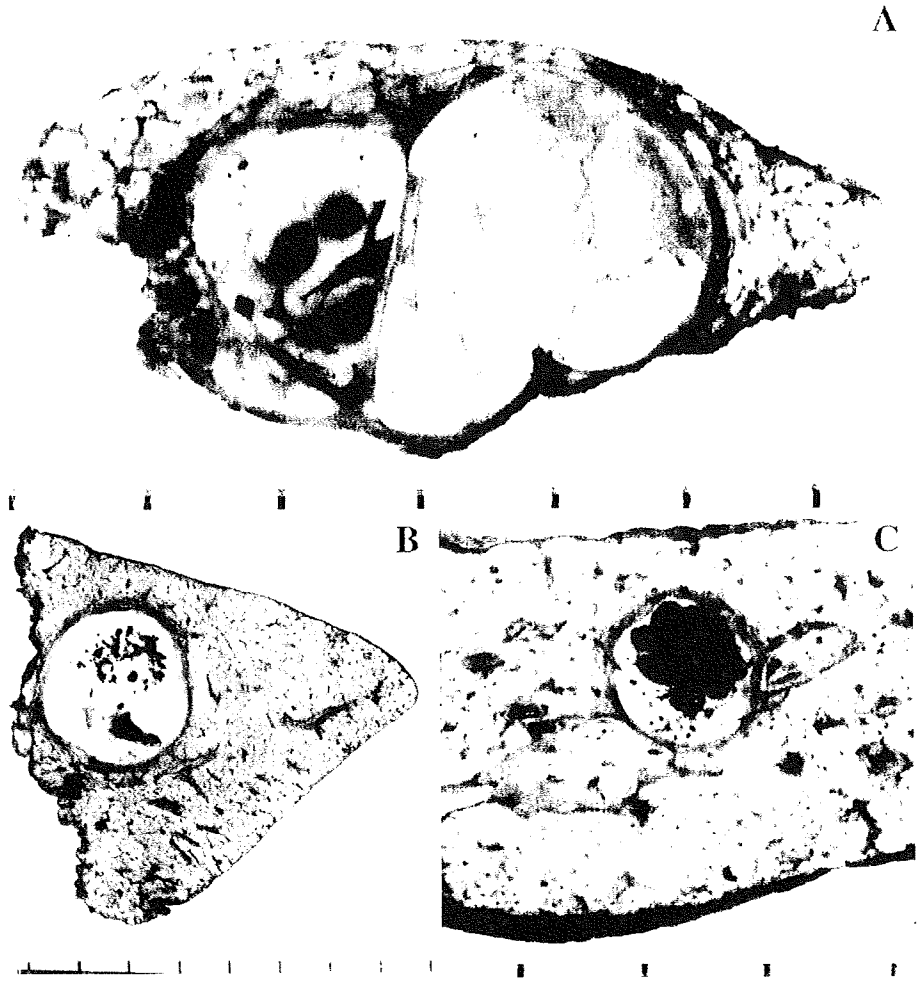

Figure 1. Macroscopic features of HCC with peliotic changes. (A) Dot-like peliotic changes. (B) Honeycomb-shaped and small blood lake-like peliotic changes in encapsulated tumor. (C) Blood lake-like peliotic change with clear boundaries occupying ~2/3 of the cut surface of the tumor.

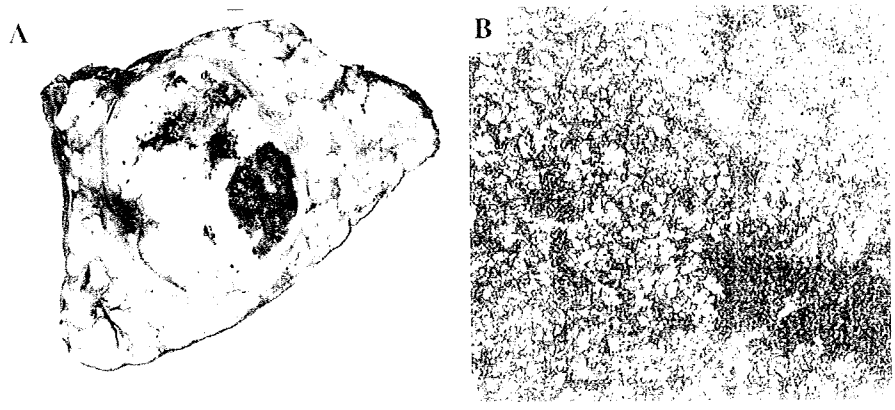

Figure 2. Hemorrhage in HCC. (A) Hemorrhage is observed in the degenerative and necrotic areas of the tumor. (B) Histologically diffuse hemorrhage is observed in degenerative HCC tissue.

tissue (Fig. 2). Fibrous septa were observed in 76 PHCCs (68%) and in 112 cases (63%) in the control group.

Peliotic change was observed as varying sized blood lakes without obvious lining of the endothelial cells (Fig. 3A). The lack of endothelial cells was also confirmed by immunostaining for CD34 (Fig. 3B). The majority of PHCCs were moderately differentiated showing a trabecular or pseudoglandular or both patterns. No well-differentiated type was found. Degeneration

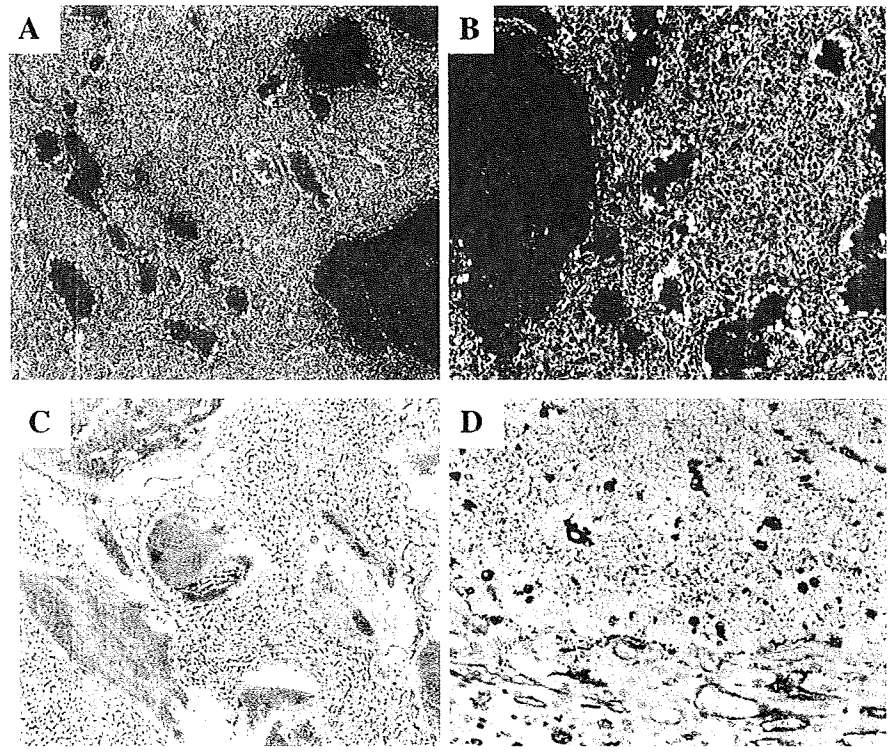

Figure 3. Histological features of peliotic changes. (A and B) Small and large blood lakes are observed in moderately differentiated HCC and irregular dilatation of sinusoid-like blood spaces of the tumor (H&E stain). (C and D) Immunostaining for CD34 shows no positive cells along the spaces of peliotic change.

or necrosis was not observed around peliotic changes. A varying degree of sinusoidal dilatation was observed around peliotic changes. In the control group, 116 tumors (66%) were moderately differentiated, 55 tumors (31%) were poorly or moderately to poorly differentiated and 6 tumors (3%) were well-differentiated. Among 111 PHCCs in which non-cancerous areas were examined, 66 cases (59%) were chronic hepatitis associated with varying degrees of fibrosis and 45 (41%) were liver cirrhosis. Among the 176 cases in the control group, 85 cases (48%) were chronic hepatitis and 91 (52%) cirrhosis. No significant difference was ntoed in the background liver between the groups.

Recurrence rate after resection. Follow-up data following surgery were obtained in 32 PHCC cases and in 39 controls. Follow-up periods ranged from 4 to 105 months (mean 38±25.7 SD). Recurrence occurred in 18 PHCC cases (56%) and in 17 controls (44%). There was no significant difference between the 2 groups.

Discussion

Peliotic changes are frequently observed in HCCs. However, the question raised is whether peliotic change is essentially different from hemorrhage of the tumor. In general, degenerative change and/or necrosis are observed around hemorrhage of HCC tumors. Put differently, degeneration and/or necrosis of tumor tissue cause hemorrhage in HCC. On the other hand, tumor tissues around peliotic changes are not degenerative or necrotic and blood is localized within the spaces. Thus, it is suggested that peliotic changes are different from hemorrhage. However, when peliotic changes become extensive, they may rupture and hemorrhage may develop.

Various factors are suggested in the pathogenesis of peliosis hepatis. These factors are excessive alcohol intake, hormonal agents such as oral contraceptives and anabolic steroids, as well as chronic wasting diseases, including malignant tumors and tuberculosis (8-12). It was also suggested that blood constituents infiltrate the Disse's spaces resulting in cyst-like change of the sinusoids following the mechanical disorder of the sinusoidal endothelial cells (13). In a study of 12 cases of peliosis hepatis, Zafrani *et al* suggested that the developmental mechanism of peliosis hepatis obstructed blood channels caused by sinusoidal destruction accompanying hepatocellular necrosis or the abnormal bonding of sinusoids and the central vein (2). Based on the fact that peliotic changes were frequently observed in the encapsulated tumors, the mechanism of peliotic change in HCC was explained by endothelial damage due to sinusoidal dilatation following increased intratumoral pressure. This assumption is supported by the fact that similar peliotic changes are frequently observed in liver cell adenoma, which is also an expansive tumor with frequent encapsulation. Sugimachi *et al* suggested a particular relationship between peliotic change in HCC and angiopoietin-2 (Ang-2), which play a regulatory role in tumor vessel remodeling (14).

No significant clinical differences were noted between the PHCC and control groups other than the significantly higher frequency of hyperechoic and/or mosaic patterns in PHCCs on ultrasonography. The most common histological feature reflecting hyperechogenecity in HCC is fatty change of the tumor which most frequently occurs in small well-differentiated tumors up to ~2 cm in diameter (15). HCC tumors with

hyperechoic and/or mosaic patterns among tumors >3-4 cm in diameter are rarely found. In the present study, these tumors proved to be PHCCs.

Although peliotic change in HCC has little clinical significance, it is necessary for clinicians and pathologists to distinguish the presence of peliotic change as a morphological feature that modifies ultrasonographic patterns of HCC.

Acknowledgements

We thank Ms. Sachiyo Maeda and Ms. Misato Shiraishi for their technical assistance on immunohistochemical staining. This study was supported in part by the Sarah Cousins Memorial Fund, Boston, MA, USA.

References

1. Karasawa T, Shikata T and Roger DS: Peliosis hepatis: report of nine cases. Acta Pathol Jpn 29: 457-469, 1979.
2. Zafrani ES, Cazier A, Baudelot AM and Feldmann G: Ultrastructural lesions of the liver in human peliosis. A report of 12 cases. Am J Pathol 114: 349-359, 1984.
3. Asano S, Wakasa H, Kaise S, Nishimaki T and Kasukawa R: Peliosis hepatis: Report of two autopsy cases with a review of literature. Acta Pathol Jpn 32: 861-877, 1982.
4. Wagner E: Fall von Blutcysten der Leber (In German). Arch Heilk 2: 369-370, 1861.
5. Kojiro M: Peliosis hepatis (In Japanese). Acta Hepatol Jpn (KANZO) 38: 583-586, 1997.
6. Grazioli L, Morana G, Caudana R, *et al*: Hepatocellular carcinoma: correlation between gadobenate dimeglumine-enhanced MRI and pathological findings. Invest Radiol 35: 25-34, 2000.
7. Brancatelli G, Baron RL, Peterson MS and Marsh W: Helical CT screening for hepatocellular carcinoma in patient with cirrhosis: frequency and cases of false-positive interpretation. Am J Roentgenol 180: 1007-1014, 2003.
8. Loomus GN, Aneja P and Bota RA: A case of peliosis hepatis in association with tamoxifen therapy. Am J Clin Pathol 80: 881-882, 1983.
9. Dejgaard A, Krogsgaard K and Jacobsen M: Veno-occlusive disease and peliosis of the liver after thorotrast administration. Virchows Arch A Pathol Anat Histopathol 403: 87-94, 1984.
10. Czapar CA, Weldon-Linne CM, Moore DM and Rhone DP: Peliosis hepatis in the acquired immunodeficiency syndrome. Arch Pathol Lab Med 110: 611-613, 1986.
11. Russmann S, Zimmermann A, Krahenbuhl S, Kern B and Reichen J: Veno-occlusive disease, nodular regenerative hyperplasia and hepatocellular carcinoma after azathioprine treatment in a patient with uncreative colitis. Eur J Gastroenterol Hepatol 13: 287-290, 2001.
12. Drevelengas A, Chourmouzi D and Boulogianni G: Peliosis of the liver in a patient with prostate carcinoma. JBR-BTR 86: 158-159, 2003.
13. Shim SG, Paik SW, Hyun JG, *et al*: Lipiodol accumulation in focal peliosis hepatis with sinusoidal dilatation. J Clin Gastroenterol 32: 356-358, 2001.
14. Sugimachi K, Tanaka S, Taguchi K, Aishima S, Shimada M and Tsuneyoshi M: Angiopoietin switching regulates angiogenesis and progression of human hepatocellular carcinoma. J Clin Pathol 56: 854-860, 2003.
15. Kutami R, Nakashima Y, Nakashima O, Shiota K and Kojiro M: Pathomorphologic study on the mechanism of fatty change in small hepatocellular carcinoma of humans. J Hepatol 33: 282-289, 2000.

Hepatology Research 2010; **40**: 330–336 doi: 10.1111/j.1872-034X.2009.00604.x

Original Article

Accelerated expression of a Myc target gene *Mina53* in aggressive hepatocellular carcinoma

Sachiko Ogasawara,[1] Mina Komuta,[2] Osamu Nakashima,[1] Jun Akiba,[1] Makoto Tsuneoka[3] and Hirohisa Yano[1]

[1]*Department of Pathology, Kurume University School of medicine, Asahi-machi, Kurume, Fukuoka,* [2]*Department of Pathology, Keio University School of medicine, Shinano-machi, Shinjuku-ku, Tokyo, and* [3]*Faculty of Pharmacy, Takasaki University of Health and Welfare, Nakaoorui-machi, Takasaki, Gunma, Japan*

Aim: Expressions of the *myc* target genes *Mina53* and *mimitin* are high in esophageal squamous cell carcinoma and colon cancer, and their relationship to cell proliferation and patient prognosis has been reported. Because *c-myc* gene expression is closely related to hepatocellular carcinoma (HCC) growth or formation and/or maintenance, we examined the *Mina53* and *mimitin* expressions in HCC.

Methods: Surgically resected 53 HCC tissues were immunohistochemically examined for *Mina53* and *mimitin* expressions and their relationship to clinicopathological factors.

Results: Diffuse *Mina53* expression was observed in the nuclei of cancer cells in the tumor nodule, but was often strong at the periphery of tumor nodules. Diffuse or scattered expression of *mimitin* was observed in the cytoplasm of HCC cells in tumor nodules. *Mina53* expression was higher in poorly differentiated HCC than in well-differentiated HCC, and significant relationship to histological grade was observed. The cases with a high *Mina53* expression also had a high expression of a proliferation marker MIB-1. This suggested the involvement of *Mina53* in cell proliferation. *Mina53* expression was high in the tumors of >2 cm of diameter than in ≤2 cm ($P < 0.01$). *Mimitin* expression tended to be high in tumors of >2 cm, but no significant relationship was observed either to histological grade, MIB-1 expression, or the other clinicopathologic factors.

Conclusions: Our findings suggested that *Mina53* expression is accelerated in HCC with a lower histological grade, with cell proliferation capability, or with a larger diameter, and *Mina53* is related to biological malignancy of HCC.

Key words: hepatocellular carcinoma (HCC), MIB-1 index, *mimitin*, *Mina53*

INTRODUCTION

HEPATOCELLULAR CARCINOMA (HCC) is one of the most common cancers worldwide and a leading cause of cancer mortality, especially in countries with a high prevalence of chronic infections with hepatitis B virus (HBV) and hepatitis C virus (HCV). The biological significance of some proto-oncogenes, tumor suppressor genes, growth factor genes and virologic factors has been implicated in hepatocarcinogenesis.[1,2] The mechanism of hepatocarcinogenesis is thought to be multifactorial that involves multiple oncogenes.[3]

Correspondence: Dr Sachiko Ogasawara, Department of Pathology, Kurume University School of Medicine, 67 Asahi-machi, Kurume, Fukuoka 830-0011, Japan. Email: sachiko@med.kurume-u.ac.jp
Received 18 May 2009; revision 21 August 2009; accepted 26 August 2009.

The *myc* family of proto-oncogenes consists mainly of 3 genes, i.e. *c-myc*, N-*myc* and L-*myc*.[4–7] Deregulated expression of *myc* family genes has been noted in many neoplastic diseases in a wide range of vertebrates including humans.[6,7] The *myc* family genes also relate to many biological phenomena besides tumorigenesis, and the genes control apoptosis and cell differentiation in addition to cell proliferation.[8,9]

c-myc is one of the most widely studied proto-oncogenes, and it is the best-characterized member in the *myc* gene-family. Generally, *c-myc* expression is associated with cell proliferation and it is down-regulated in quiescent and differentiated cells.

Recently, Tsuneoka *et al.* identified the novel genes, *Mina53* (*myc*-induced nuclear antigen)[10] and *mimitin* (*myc*-induced mitochondria protein),[11] and presented that *c-myc* directly induced their expressions. The *Mina53* gene encodes a protein with a molecular weight of 53 kDa that is localized in nucleus and with part of

the protein concentrated in the nucleolus. The *mimitin* gene encodes a protein with a molecular weight of 20 kDa that is localized in mitochondria. *Mina53* expression was reported in esophageal squamous cell carcinoma (ESCC)[12] and colon cancer,[13] the expression was high in poor prognostic cases of ESCC, and its relationship to cell proliferation has been indicated. *Mimitin* expression was also reported in ESCC, and its relationship to cell proliferation was shown.[11] However, their functions are not yet fully clarified, and there have been no studies on them in the tissues level of hepatocytes. Because *c-myc* gene expression is closely related to HCC growth or formation and/or maintenance,[14–16] we examined the relationship between *Mina53* and *mimitin* expressions in HCC tissues and clinicopathological factors.

MATERIALS AND METHODS

TISSUE SAMPLES OF HCC and non-HCC were obtained from 53 patients who underwent surgical resection of tumors in the Kurume University Hospital and its affiliated hospitals in the period between 1994 and 1996. Before the surgery, none of these patients had received any form of treatment such as arterial embolization and chemotherapy. Histologically, the 53 surgically obtained samples consisted of 6 well+moderately differentiated HCCs, 35 moderately differentiated HCCs, 9 moderately+poorly differentiated HCCs and 3 poorly differentiated HCCs. Non-cancerous area presented liver cirrhosis ($n = 23$) or chronic hepatitis ($n = 30$).

The HCC specimens were immunohistochemically stained and examined for the relationship between the expressions of *Mina53* or *mimitin* and such clinicopathologic factors as histological grade of HCC, capsule formation, capsule infiltration, tubular invasion, recurrence rate, survival rate, and histological change in non-HCC tissues (normal, hepatitis, liver cirrhosis).

For immunohistochemical examinations, the surgically obtained tissue samples were formalin fixed and paraffine embedded by using the usual procedure. Serial sections 4-μm thick were mounted on coated slides and deparaffinized in xylene and graded alcohol. The sections were soaked in Target Retrieval Solution (Dako, Carpinteria, CA), and treated in a microwave oven for 30 min. Mouse monoclonal anti-*Mina53* antibody (concentration: 3.4 μg/mL) and rabbit polyclonal anti-*mimitin* antibody (concentration: 0.7 μg/mL) were established at Division of Human Genetic Department of Forensic Medicine, Kurume University School of Medicine and specificity of these antibodies was confirmed in previous studies.[10,11] Ki-67 antibody (clone MIB-1, concentration: 0.8 μg/mL) was obtained from Dako A/S (Glostrup). The sections were incubated with primary antibodies for 60 min at room temperature. Immunohistochemical staining was performed using CSA II (Dako) according to the manufacturer's protocol. The peroxidase reaction was developed with the substrate 3,3-diaminobenzidine and H_2O_2. After light counterstaining with hematoxylin, the slides were dehydrated, coverslipped, and observed under a microscope.

By examining the cancerous tissues, the specimens were classified into 3 groups according to the percentage of HCC cells that were immunohistochemically positive to *Mina53* and *mimitin*, i.e. negative (−) if 0%, low-expression (+) if 1–33%, high-expression (++) if 34%<.

The Ki-67 staining results (MIB-1 index) of tumor cells were evaluated in the following manner: In the *Mina53*- or *mimitin*-positive samples, MIB-1 index in the area that contained *Mina53*- or *mimitin*-positive cells and presented the highest MIB-1 expression level was evaluated. In the *Mina53*- or *mimitin*-negative samples, MIB-1 index in the area with the highest MIB-1 expression level was evaluated. Total number of stained cells was estimated as the sum of positive and negative tumor cells, and then the ratio of positive cell number to the estimated total cell number was obtained. The average MIB-1 index in our specimens was 28.2%, and the specimens were classified into two groups (≤28% and 28%<).

Statistics

The Mann–Whitney *U*-test was used to examine the relationship between known prognostic factors and the expression level of *Mina53* or of *mimitin*, and MIB-1 index. The Kaplan–Meier method was used to calculate disease-free survival rate. All statistical analyses were performed with StatMate III (ATMS, Tokyo). *P*-values less than 0.05 were considered statistically significant.

RESULTS

Immunohistochemistry

MINA53 EXPRESSION WAS detected in the nuclei of HCC cells in tumor nodule and in portal vein tumor thrombi. The expression was observed diffusely in tumor nodules, but it was often strong HCC cells at the periphery of tumor nodules (Fig. 1a,b). The expression was also observed in lymphocytes infiltrating into the capsules (data not shown). In non-cancerous tissues,

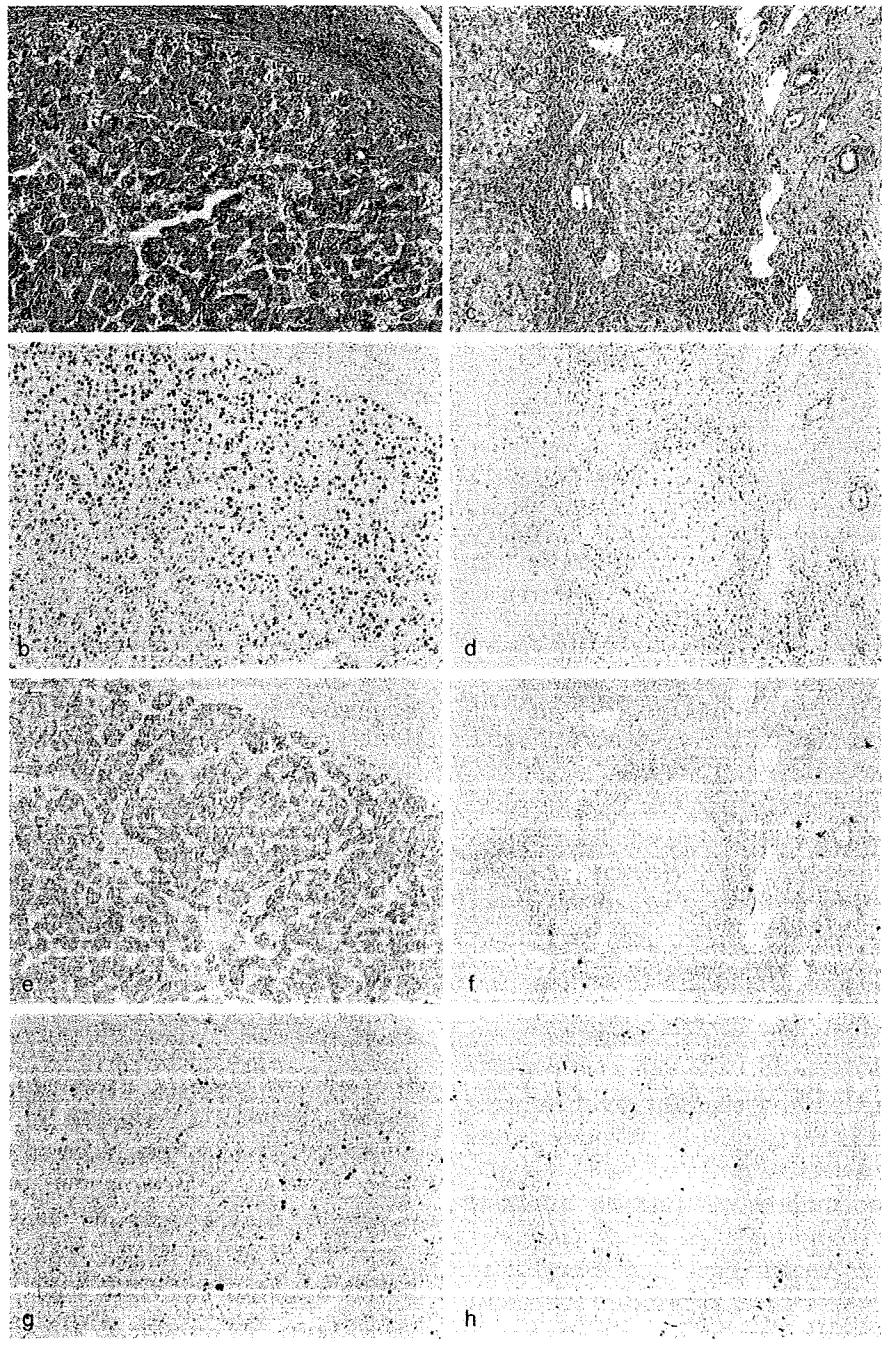

Figure 1 Immunohistochemical staining of *Mina53*, *mimitin* and MIB-1 in hepatocellular carcinoma (HCC) and non-cancerous tissues. (a) Moderately differentiated HCC (hematoxylin & eosin staining, ×100). (b) *Mina53* expression in the nuclei of cancer cells. HCC cells at the periphery of tumor nodule show stronger expression (×100). (c) Non-cancerous area (hematoxylin & eosin staining, ×100). (d) *Mina53* expression was observed in the nuclei of bile duct epithelium, of some of the lymphocytes in a portal area, and of hepatocytes around portal areas (×100). (e) Diffuse *mimitin* expression in the cytoplasm of HCC cells (×100). (f) *Mimitin* expression in bile duct epithelium and some cells in portal areas (×100). (g) MIB-1 expression in the nuclei of cancer cells of tumor nodule (×100). (h) MIB-1 expression in non-HCC tissue (×100).

Table 1 Relationship between clinicopathological factors and *Mina53* expression in hepatocellular carcinoma ($n = 53$)

Mina53 expression level		–	+	++
Histological grade*:				
Well+moderately differentiated		3	3	0
Moderately differentiated		8	12	15
Moderately+poorly differentiated		0	2	7
Poorly differentiated		0	1	2
MIB-1 index (%)**:	≤28	11	12	5
	>28	0	6	19
Tumor diameter***:	≤2 cm	6	2	1
	>2 cm	5	16	23
Capsule formation:	Present	11	16	20
	Absent	0	2	4
Capsule invasion:	Present	11	15	20
	Absent	0	3	4
Portal vein invasion:	Present	5	7	14
	Absent	6	11	10
Non-cancerous tissue:	Liver cirrhosis	6	10	7
	Chronic hepatitis	5	8	17
Intrahepatic metastasis:	Present	1	6	8
	Absent	10	12	16

–: negative. +: low-expression. ++: high-expression. *$P < 0.05$. **$P < 0.001$. ***$P < 0.01$.

Mina53 expression was observed in the nuclei of bile duct epithelium and of some of the lymphocytes infiltrating into portal areas. *Mina53* expression was also observed in compressed hepatocytes just around tumor nodules, and in those around portal areas when active interface hepatitis was present (Fig. 1c,d).

Diffuse or sometimes scattered expression of *mimitin* was often observed in the cytoplasm of HCC cells in tumor nodules (Fig. 1e). Non-cancerous tissues expressed *mimitin* in bile duct epithelium, and in scattered round cells in portal areas or fibrous areas (Fig. 1f). Some of the latter cells had Giemsa stain-positive granules in the cytoplasm, suggesting they are mast cells.

The positive cell area and intensity of *Mina53* or *mimitin* expression were larger and higher, respectively, in HCC cells than in non-HCC tissues.

Strong MIB-1 expression was often observed in the nuclei of HCC cells at the periphery of tumor nodules (Fig. 1g), and some cases had the expression in portal vein tumor thrombi (data not shown). In non-cancerous tissues, MIB-1 was expressed in the hepatocytes around tumor nodules and periphery of regenerative nodules (Fig. 1h), bile duct epithelium, and lymphocytes around portal areas.

Mina53 and MIB-1 expressions were localized in the nuclei, but in both cancerous and non-cancerous tissues of most cases, *Mina53* expression was higher than MIB-1.

Mina53 expression and clinicopathological factors (Table 1)

Mina53 expression level was negative (–) in 11 cases (20.7%, 3 well+moderately differentiated cases and 8 moderately differentiated cases), low-expression (+) in 18 cases (34.0%, 3 well+moderately differentiated, 12 moderately differentiated, 2 moderately+poorly differentiated, and one poorly differentiated), and high-expression (++) in 24 cases (45.3%, 15 moderately differentiated, 7 moderately+poorly differentiated, and 2 poorly differentiated). *Mina53* expression was weak in well-differentiated HCCs and strong in poorly differentiated HCCs. Statistically significant difference among the 3 expression levels was observed ($P < 0.05$).

MIB-1 index was low in the cases with weak *Mina53* expressions, high in cases with strong *Mina53* expressions, and the statistical significance ($P < 0.001$) was obtained.

Tumor diameter was ≤2 cm in many cases with weak *Mina53* expressions, while it was >2 cm in many cases with strong expression. Number of cases with >2 cm of diameter increased along with the increase in *Mina53* expression level, and the statistical significance

Table 2 Relationship between clinicopathological factors and *mimitin* expression in hepatocellular carcinoma ($n = 53$)

Mimitin expression level		–	+	++
Histological grade:				
Well+moderately differentiated		1	4	1
Moderately differentiated		7	11	17
Moderately+poorly differentiated		1	3	5
Poorly differentiated		1	1	1
MIB-1 index (%):	≤28	7	10	14
	>28	3	9	10
Tumor diameter:	≤2 cm	3	2	3
	>2 cm	7	17	21
Capsule formation:	Present	10	15	22
	Absent	0	4	2
Capsule invasion:	Present	10	14	22
	Absent	0	5	2
Portal vein invasion:	Present	4	10	12
	Absent	6	9	12
Non-cancerous tissue:	Liver cirrhosis	3	8	12
	Chronic hepatitis	7	11	12
Intrahepatic metastasis:	Present	0	8	7
	Absent	10	11	17

–: negative. +: low-expression. ++: high-expression.

($P < 0.01$) was obtained between the 3 expression level groups.

Frequency of portal vain invasion was tended to be high in the cases with strong *Mina53* expression, but there was no significant difference. Statistical significance was not observed either between *Mina53* expression and capsule formation, capsule invasion, or background diseases in non-cancerous tissues.

Mimitin expression and clinicopathological factors (Table 2)

Mimitin expression was negative (–) in 10 cases (18.9%, one well+moderately differentiated case, 7 moderately differentiated cases, one moderately+poorly differentiated case and one poorly differentiated case), low-expression (+) in 19 cases (35.8%, 4 well+moderately differentiated, 11 moderately differentiate, 3 moderately+poorly differentiated and one poorly differentiated), and high-expression (++) in 24 cases (45.3%, one well+moderately differentiated, 17 moderately differentiated, 5 moderately+poorly differentiated, and one poorly differentiated).

No significant differences were obtained between *mimitin* expression and histological grade or MIB-1 index.

Average tumor diameter increased from 32.9 mm in the negative expression group to 42.6 mm in the low-expression group, and 43.7 mm in the high-expression group, but there was no significant difference. There were no significant relationships to the other clinicopathological factors such as capsule formation and capsule invasion.

DISCUSSION

IMMUNOHISTOCHEMICAL STAININGS FOR *Mina53*, *mimitin* and MIB-1 were conducted on 53 HCC cases, and the relationship between their expressions and clinicopathological factors were examined.

Mina53 expression was reported to have a relationship with MIB-1 (an immunohistochemical proliferation marker) index in esophageal and colonic cancer tissues,[12,13] and suppression of *Mina53* expression *in vitro* by *Mina53*-specific small interfering RNA (siRNA) suppressed proliferation of esophageal and colorectal cancer cell lines. In the human colon cancer cell line SW620, suppression of *c-myc* expression by *c-myc*-specific siRNA suppressed *Mina53* expression, and this suggested direct involvement of *c-myc* in *Mina53* expression.[13]

To date, *Mina53* expression in HCC was not reported in the tissues level, but the relationships between *c-myc* and HCC were studied, e.g. *c-myc* expression is higher in HCC than normal liver,[17] higher in HCC with a large diameter or high proliferative capability,[18] and higher in HCC with multiple nodules than with single nodule.[19]

In our present immunohistochemical study, the positive cell area and intensity of *Mina53* expression were smaller and lower, respectively, in non-neopastic cells than HCC cells.

In HCC tissues, *Mina53* expression was observed diffusely in cancer cells in tumor nodules, and it was often observed strongly in HCC cells at the periphery of tumor nodules, and the expression level was related to MIB-1 index. In addition, the expression level was high in HCC at a low histological level and in HCC that diameter was >2 cm. We examined *Mina53* expression in 5 cases of HCC showing "nodule-in-nodule" appearance and found the strongest expression in less-differentiated HCC tissues in the central area (data not shown). These findings suggest that *Mina53* expression is related to biological malignancy and cell proliferation in HCC. In colon cancer tissues, *Mina53* expression was higher than MIB-1 expression,[13] and a similar tendency was observed in our HCC cases with *Mina53* expressions.

In non-HCC tissues, *Mina53* and MIB-1 were expressed in hepatocytes at the periphery of regenerative nodules and in compressed hepatocytes, but *Mina53* expression was higher than MIB-1. Bile duct epithelium and some of the lymphocytes express *Mina53*, but do not expresse MIB-1. In the non-cancerous region of renal cell carcinoma, *Mina53* was diffusely positive in normal tubules, but MIB-1 was generally negative.[20] In the non-cancerous tissues of esophageal carcinoma, *Mina53* expressions were found in the layers from the basal to the suprabasal, while MIB-1 expressions were found in the basal or epibasal areas.[12] In non-cancerous tissues of colon cancer, MIB-1 was expressed in the normal cells of crypt and lymphoid germinal center, while *Mina53* expressions were only sometimes observed.[13] These data suggest that in non-cancerous areas, *Mina53* expressions does not always coincide with MIB-1 expressions, and may not be regarded as having the same function as that of involvement in cancer cell proliferation as we previously speculated.[20]

MIB-1 is expressed during G1, S, G2 and M phases of cell cycle.[21–23] *Mina53* is a *myc*-target gene, and *c-myc* is expressed continuously in all phases of cell cycle in proliferating cells.[13] However, *Mina53* expression induced by *c-myc* is thought to occur in the proliferation of specific cells.

Relationship between *Mina53* expression and survival rate was studied in esophageal squamous cell carcinoma (ESCC),[12] renal cell carcinoma,[20] and neuroblastoma.[24] These studies reported higher survival rates in the cases with low *Mina53* expressions. However, our findings in this current study did not show significant relationship between *Mina53* expression and survival rate. On the other hand, relationship between *c-myc* expression and recurrence was observed in HCC,[18] but not in our findings.

In ESCC and other cancerous tissues, *Mina53* expression was involved to cell proliferation and related to survival rate and MIB-1 index, but *Mina53* expression and MIB-1 expression in non-cancerous area of cancerous tissues varied between studies. This suggested that *Mina53* is not a single regulative factor in cell proliferation, but various factors together with *Mina53* are involved in proliferation.

MIB-1 index increased with the progress of disease conditions, i.e. from normal liver tissues, hepatitis, liver chirrhosis, and then to HCC.[25] MIB-1 index is also reported to have a relationship to clinicopathological factors of HCC such as histological grade, survival rate, intrahepatic metastasis;[26] and to the HCC marker PIVKA-II, β-catenin that takes a role in cell-cell adhesion,[27] and ubiquitin that involves to protein repair and proteolysis.[28] In our current study, significant relationship was observed between MIB-1 index and such clinicopathological factors as histological grade, tumor diameter and intrahepatic metastasis, but not with survival rate and recurrence rate. King *et al.*[29] and Schmitt-Graff *et al.*[25] also examined survival and recurrence rates for ≥10% or <10% of MIB-1 levels, and they only indicated a possible relationship between patient prognosis and MIB-1 index. Grouping of MIB-1 index levels would need further investigation.

Suppression of *mimitin* expression in the ESCC cell line TE-11 by using *mimitin*-specific siRNA suppressed cell proliferation.[11] In ESCC tissues, *mimitin* was highly expressed, and the expression level was significantly correlated with the increase of MIB-1 index, but not with histological grade or age of patients.[11]

In HCC tissues of our current study, *mimitin* was expressed in varying degrees, but the expression was not correlated with cell proliferation as shown in ESCC, and it was not correlated with such clinicopathological factors as histological grade and tumor diameter.

In our current study, *Mina53* expression was more closely related to clinicopathological factors than *mimitin* expression. Tsuneoka *et al.* reported that the suppression of *mimitin* by using *mimitin*-specific siRNA in the HCC cell line KYN-2 did not inhibit cell proliferation.[11] These findings suggest that *Mina53* is more closely related to cell proliferation in HCC than *mimitin*.

Better understanding of *myc*-family gene expressions would help better management of neoplastic diseases. Identification and characterization of *myc*-specific target

genes such as *Mina53* and *mimitin* would help control cell proliferation, and open up a new frontier in cancer treatment.

REFERENCES

1 Tabor E. Tumor suppressor genes, growth factor genes, and oncogenes in hepatitis B virus-associated hepatocellular carcinoma. *J Med Virol* 1994; 42: 357–65.
2 Caselmann WH. Transactivation of cellular gene expression by hepatitis B viral proteins: a possible molecular mechanism of hepatocarcinogenesis. *J Hepatol* 1995; 22: 34–7.
3 Rogler CE, Chisari FV. Cellular and molecular mechanisms of hepatocarcinogenesis. *Semin Liver Dis* 1992; 12: 265–78.
4 Marcu KB, Bossone SA, Patel AJ. Myc function and regulation. *Annu Rev Biochem* 1992; 61: 809–60.
5 Morgenbesser SD, DePinho RA. Use of transgenic mice to study myc family gene function in normal mammalian development and in cancer. *Semin Cancer Biol* 1994; 5: 21–36.
6 Henriksson M, Luscher B. Proteins of the Myc network: essential regulators of cell growth and differentiation. *Adv Cancer Res* 1996; 68: 109–82.
7 Grandori C, Cowley SM, James LP, Eisenman RN. The Myc/Max/Mad network and the transcriptional control of cell behavior. *Annu Rev Cell Dev Biol* 2000; 16: 653–99.
8 Lutz W, Leon J, Eilers M. Contributions of Myc to tumorigenesis. *Biochim Biophys Acta* 2002; 1602: 61–71.
9 Tsuneoka M, Ras MekadaE. /MEK signaling suppresses Myc-dependent apoptosis in cells transformed by c-myc and activated ras. *Oncogene* 2000; 19: 115–23.
10 Tsuneoka M, Koda Y, Soejima M, Teye K, Kimura H. A novel myc target gene, *Mina53*, that is involved in cell proliferation. *J Biol Chem* 2002; 277: 35450–9.
11 Tsuneoka M, Teye K, Arima N *et al.* A novel Myc-target gene, *mimitin*, that is involved in cell proliferation of esophageal squamous cell carcinoma. *J Biol Chem* 2005; 280: 19977–85.
12 Tsuneoka M, Fujita H, Arima N *et al. Mina53* as a potential prognostic factor for esophageal squamous cell carcinoma. *Clin Cancer Res* 2004; 10: 7347–56.
13 Teye K, Tsuneoka M, Arima N *et al.* Increased expression of a Myc target gene *Mina53* in human colon cancer. *Am J Pathol* 2004; 164: 205–16.
14 Yaswen P, Goyette M, Shank PR, Fausto N. Expression of c-Ki-ras, c-Ha-ras, and c-myc in specific cell types during hepatocarcinogenesis. *Mol Cell Biol* 1985; 5: 780–6.
15 Thompson NL, Mead JE, Braun L, Goyette M, Shank PR, Fausto N. Sequential protooncogene expression during rat liver regeneration. *Cancer Res* 1986; 46: 3111–17.
16 Zhang XK, Huang DP, Qiu DK, Chiu JF. The expression of c-myc and c-N-ras in human cirrhotic livers, hepatocellular carcinomas and liver tissue surrounding the tumors. *Oncogene* 1990; 5: 909–14.
17 Arbuthnot P, Kew M, Fitschen W. c-fos and c-myc oncoprotein expression in human hepatocellular carcinomas. *Anticancer Res* 1991; 11: 921–4.
18 Kawate S, Fukusato T, Ohwada S, Watanuki A, Morishita Y. Amplification of c-myc in hepatocellular carcinoma: correlation with clinicopathologic features, proliferative activity and p53 overexpression. *Oncology* 1999; 57: 157–63.
19 Wang Y, Wu MC, Sham JS, Zhang W, Wu WQ, Guan XY. Prognostic significance of c-myc and AIB1 amplification in hepatocellular carcinoma. A broad survey using high-throughput tissue microarray. *Cancer* 2002; 95: 2346–52.
20 Ishizaki H, Yano H, Tsuneoka M *et al.* Overexpression of the myc target gene *Mina53* in advanced renal cell carcinoma. *Pathol Int* 2007; 57: 672–80.
21 Gerdes J, Lemke H, Baisch H, Wacker HH, Schwab U, Stein H. Cell cycle analysis of a cell proliferation-associated human nuclear antigen defined by the monoclonal antibody Ki-67. *J Immunol* 1984; 133: 1710–15.
22 Lopez F, Belloc F, Lacombe F *et al.* Modalities of synthesis of Ki67 antigen during the stimulation of lymphocytes. *Cytometry* 1991; 12: 42–9.
23 Bruno S, Darzynkiewicz Z. Cell cycle dependent expression and stability of the nuclear protein detected by Ki-67 antibody in HL-60 cells. *Cell Prolif* 1992; 25: 31–40.
24 Fukahori S, Yano H, Tsuneoka M *et al.* Immunohistochemical expressions of Cap43 and *Mina53* proteins in neuroblastoma. *J Pediatr Surg* 2007; 42: 1831–40.
25 Schmitt-Graff A, Ertelt V, Allgaier HP *et al.* Cellular retinol-binding protein-1 in hepatocellular carcinoma correlates with beta-catenin, Ki-67 index, and patient survival. *Hepatology* 2003; 38: 470–80.
26 Morinaga S, Ishiwa N, Noguchi Y *et al.* Growth index, assessed with Ki-67 and ssDNA labeling; a significant prognosticator for patients undergoing curative resection for hepatocellular carcinoma. *J Surg Oncol* 2005; 92: 331–6.
27 Inagawa S, Itabashi M, Adachi S *et al.* Expression and prognostic roles of beta-catenin in hepatocellular carcinoma: correlation with tumor progression and postoperative survival. *Clin Cancer Res* 2002; 8: 450–6.
28 Shirahashi H, Sakaida I, Terai S, Hironaka K, Kusano N, Okita K. Ubiquitin is a possible new predictive marker for the recurrence of human hepatocellular carcinoma. *Liver* 2002; 22: 413–18.
29 King KL, Hwang JJ, Chau GY *et al.* Ki-67 expression as a prognostic marker in patients with hepatocellular carcinoma. *J Gastroenterol Hepatol* 1998; 13: 273–9.